

Ultrastable Radical-doped Coordination Compounds with Antibacterial Activity against Antibiotic -Resistant Bacteria

Hua Ke,^[a,b]† Fen Hu,^[c]† Lingyi Meng,^[b] Qi-Hua Chen,^[a] Qian-Sheng Lai,^[a] Ze-Chen Li,^[a] Ze-Long Huang,^[c] Jian-Zhen Liao,^{*[a,b]} Jian-Ding Qiu^{*[a]} and Can-Zhong Lu^{*[b]}

^a Engineering Technology Research Center for Environmental Protection Materials, Pingxiang University, Pingxiang, Jiangxi 337055 (PR China); E-mail: jianzhenliao@sina.com; jdqiu@ncu.edu.cn

^b Key Laboratory of Design and Assembly of Functional Nanostructures, Fujian Provincial Key Laboratory of Nanomaterials, Fujian Institute of Research on the Structure of Matter, Chinese Academy of Sciences, Fuzhou, Fujian, 350002, P. R. China. E-mail: czlu@fjirsm.ac.cn.

^c Key Laboratory of Gastrointestinal Cancer (Fujian Medical University), Ministry of Education, School of Basic Medical Sciences, Fujian Medical University, Fuzhou, Fujian 350002 (PR China)

† These authors contributed equally to this work.

Table of Contents

1. Materials and Physical Measurements
2. Experimental Section
3. Single Crystal X-ray Diffraction Analyses
4. Crystal Data for Compounds 1 and 2
5. X-ray Powder Diffraction
6. UV-Vis Diffuse Reflection Spectroscopy
7. Computational Studies
8. Antibacterial Activity Measurement
9. Thermogravimetric Analyses
10. References

1. Materials and Physical Measurements

All chemicals were obtained from commercial sources and used as received without further purification. Powder X-ray diffraction (PXRD) were collected on Rigaku desktop MiniFlex 600 diffractometer with Cu K α radiation ($\lambda=1.5418$ Å). FT-IR spectra were recorded in the range 4000–400 cm⁻¹ on a Perkin-Elmer FT-IR spectrum 2000 spectrometer with pressed KBr pellets. Optical diffuse reflectance spectra were measured at room temperature on a Perkin Elmer Lambda-950 UV/Vis/NIR spectrophotometer. ESR spectra were recorded on a Bruker BioSpin E500 ESR spectrometer with a 100 KHz magnetic field modulation at room temperature equipped with an UV light source (16 mW). The morphology of the bacteria was imaged by a scanning electron microscope (SEM, Hitachi SU-8010). Thermal analyses were performed on a TGA/DSC 1 STAR^e system from room temperature to 800°C with a heating rate of 10 K/min under nitrogen.

2. Experimental Section

Synthesis of N, N'-di(ethanesulfonic acid)-1,4,5,8-naphthalenediimide (H₂TauNDI). The ligand was synthesized according to the procedure in reference. ^[S1] A mixture of 1,4,5,8-naphthalene-tetracarboxylic dianhydride (NDA) (1.41 g, 5.26 mmol) and taurine (1.316 g, 10.52 mmol) in DMF (65 mL) was heated under 423K for about 19 h. When the reaction mixture reached room temperature, a light yellow crystalline solid precipitated out, which was collected by filtration.

Synthesis of compound 1. A mixture of H₂TauNDI (0.0480 g, 0.1 mmol), KNO₃ (0.0101 g, 0.1 mmol), H₂O (3 mL), and EtOH (1 mL) were heated in a 20 mL brown Vial at 95°C for 3 days, followed by programmed cooled for 1 day to room temperature. After suction filtration, the faint yellow crystals were collected. Yield: 41% (based on K). FT-IR (cm⁻¹): 3609(m), 3508(w), 3077(m), 1700(s), 1664(s), 1582(m), 1449(s), 1347(s), 1187(s), 1041(s), 903(w), 811(m), 765(m), 633(m), 532(s).

Synthesis of compound 2. A mixture of H₂TauNDI (0.0480 g, 0.1 mmol), Ca(NO₃)₂ (0.0241 g, 0.1 mmol), H₂O (2 mL), and EtOH (3 mL) were heated in a 25 mL Teflon-lined autoclave at 80°C for 3 days, followed by programmed cooled for 1 day to room temperature. After suction filtration, the faint yellow crystals were collected. Yield: 49% (based on Ca). FT-IR (cm⁻¹): 3495(m), 1702(s), 1656(s), 1583(m), 1463(m), 1380(m), 1344(s), 1270(m), 1248(m), 1216(m), 1188(s), 1070(s), 1018(m), 876(w), 826(w), 766(s), 642(m), 537(s).

3. Crystallographic Data Collection and Refinement

A suitable crystal of compound **1** or **2** was selected and collected on a XtaLAB Synergy R, HyPix diffractometer. The crystal was kept at 293(2) K during data collection. Using Olex2^[S2], the

structure was solved with the ShelXS ^[53] structure solution program using Direct Methods and refined with the ShelXL ^[54] refinement package using Least Squares minimisation. Crystallographic data has been deposited at the Cambridge Crystallographic Data Center with reference number CCDC 2032620, 2032621. These data can be obtained free of charge from The Cambridge Crystallographic Data Centre via http://www.ccdc.cam.ac.uk/data_request/cif.

4. Crystal Data for Compounds 1 and 2

Crystal Data for compound **1** ($M = 576.63$ g/mol): triclinic, space group P-1 (no. 2), $a = 5.62440(10)$ Å, $b = 6.10970(10)$ Å, $c = 15.9088(3)$ Å, $\alpha = 89.883(2)^\circ$, $\beta = 81.215(2)^\circ$, $\gamma = 76.999(2)^\circ$, $V = 526.121(17)$ Å³, $Z = 1$, $T = 293(2)$ K, $\mu(\text{CuK}\alpha) = 6.473$ mm⁻¹, $D_{\text{calc}} = 1.820$ g/cm³, 5054 reflections measured ($5.624^\circ \leq 2\theta \leq 149.744^\circ$), 2063 unique ($R_{\text{int}} = 0.0214$, $R_{\text{sigma}} = 0.0222$) which were used in all calculations. The final R_1 was 0.0389 ($I > 2\sigma(I)$) and wR_2 was 0.1166 (all data).

Crystal Data for compound **2** ($M = 556.53$ g/mol): monoclinic, space group P2₁/n (no. 14), $a = 8.8177(3)$ Å, $b = 28.7454(7)$ Å, $c = 8.9688(3)$ Å, $\beta = 108.766(3)^\circ$, $V = 2152.46(11)$ Å³, $Z = 4$, $T = 293(2)$ K, $\mu(\text{CuK}\alpha) = 4.992$ mm⁻¹, $D_{\text{calc}} = 1.717$ g/cm³, 14444 reflections measured ($6.15^\circ \leq 2\theta \leq 150.346^\circ$), 4269 unique ($R_{\text{int}} = 0.0526$, $R_{\text{sigma}} = 0.0465$) which were used in all calculations. The final R_1 was 0.0583 ($I > 2\sigma(I)$) and wR_2 was 0.1681 (all data).

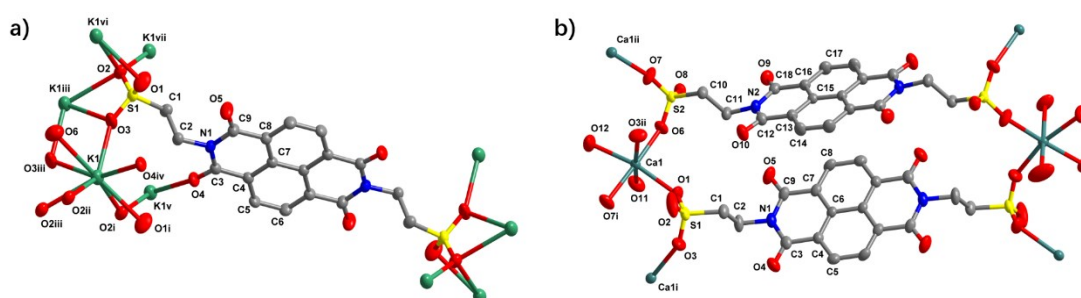


Figure S1. (a) View of the coordination environment of the K cations in **1** with the thermal ellipsoids drawn at 30% probability level. Symmetry code: i) $x, 1+y, z$; ii) $-1+x, 1+y, z$; iii) $-x, 1-y, 1-z$; iv) $-1+x, y, z$; v) $1+x, y, z$; vi) $x, -1+y, z$; vii) $1+x, -1+y, z$. (b) View of the coordination environment of the Ca cations in **2** with the thermal ellipsoids drawn at 30% probability level. Symmetry code: i) $-0.5+x, 0.5-y, -0.5+z$; ii) $0.5+x, 0.5-y, 0.5+z$. All hydrogen atoms are omitted for clarity.

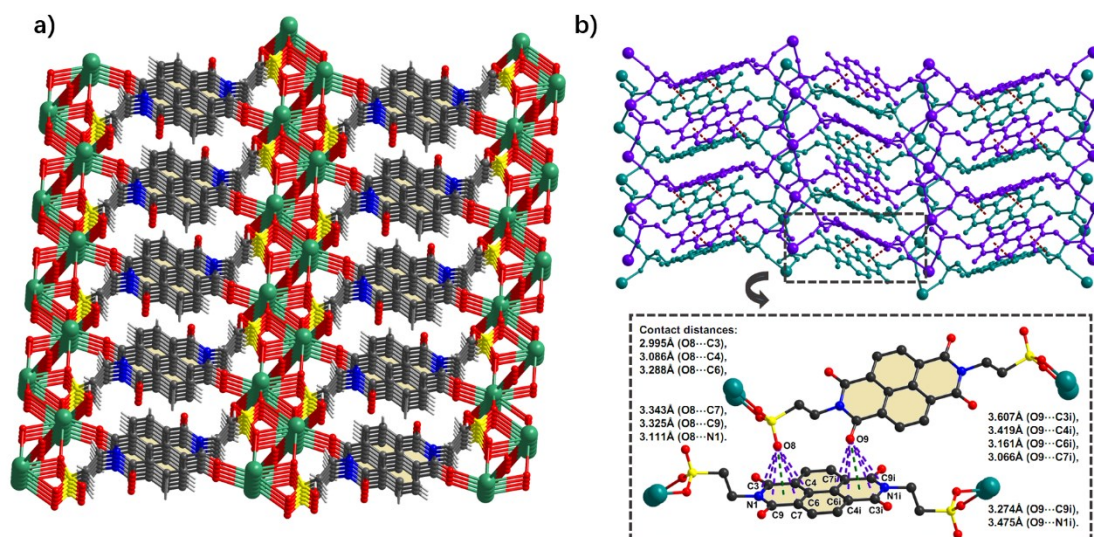


Figure S2. (a) View of three dimensional structure of compound **1**; (b) Adjacent layers in compound **2** connected with each other by moderate lone pair- π interactions; the O...ring distances are listed above, varying from 2.995 to 3.607 Å (Dotted line: lone pair- π interactions).

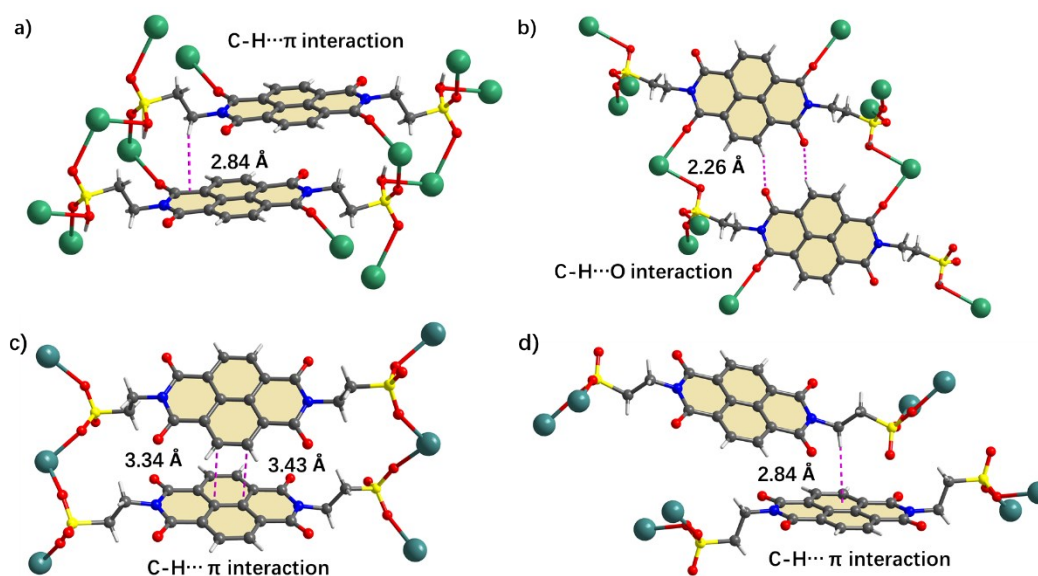


Figure S3. The intramolecular C-H... π interactions and C-H...O hydrogen bonds in compound **1** (a-b) and intramolecular C-H... π interactions in **2** (c-d).

Table S1 Hydrogen-bond Geometry (Å, °) for Compound **1**

D—H...A [#]	[Symmetry code]	d(D—H)	d(H...A)	d(D...A)	∠DHA
C1—H1B...O4	x, -1+y, z	0.97	2.52	3.350(3)	144
C2—H2B...O4	-	0.97	2.39	2.728(3)	100
C6—H6...O5	1+x, 1+y, z	0.93	2.26	3.137(3)	158

[#] D = Donor, A = Acceptor.

Table S2 Hydrogen-bond Geometry (Å, °) for Compound **2**

D—H...A [#]	[Symmetry code]	d(D—H)	d(H...A)	d(D...A)	∠DHA
----------------------	-----------------	--------	----------	----------	------

O11—H11C…O4	$x, y, 1+z$	0.91	1.97	2.857(6)	164
O11—H11D…O2	$-1/2+x, 1/2-y, 1/2+z$	0.90	1.81	2.680(4)	163
O12—H12C…O11	$1/2+x, 1/2-y, 1/2+z$	0.94	1.95	2.864(8)	165
O12—H12D…O10	$-1/2+x, 1/2-y, 1/2+z$	0.88	1.95	2.829(1)	173
C11—H11B…O8	-	0.99	2.59	3.058(6)	109
C11—H11B…O9	-	0.99	2.39	2.752(9)	101
C14—H14…O8	$x, y, -1+z$	0.95	2.55	3.098(7)	117

D = Donor, A = Acceptor.

5. X-ray Powder Diffraction

The phase purities of the compounds are convincingly established by comparison of the powder X-ray diffraction patterns of the as-synthesized products with the simulated ones from the single-crystal data. The PXRD patterns for compound **1** or **2** before irradiation and that after irradiation by LED light with power of 3 W (460-465 nm) are in accordance with the simulated PXRD pattern one, indicating the crystal structure of **1** or **2** were left unchanged during the color change.

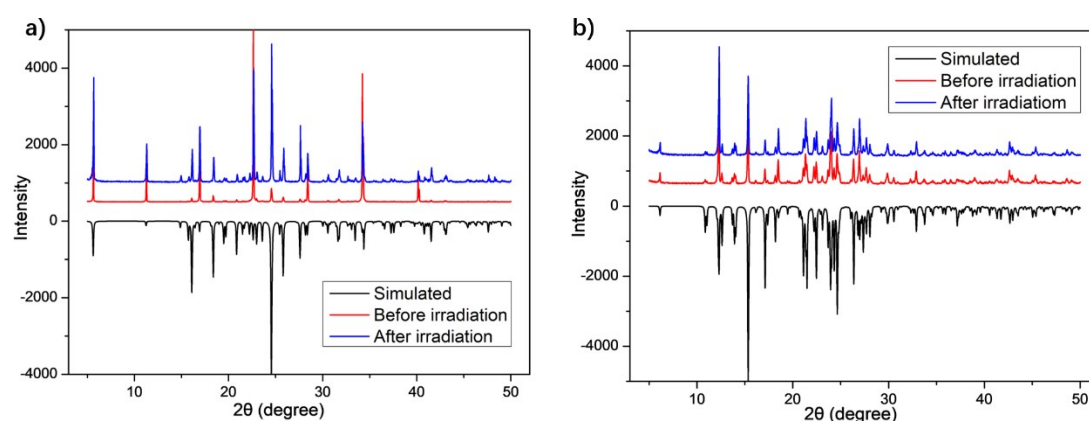


Figure S4. (a) The simulated PXRD pattern based on the single crystal **1**, the as-synthesized and that after irradiated by LED light with the power of 3 W (460-465 nm). (b) The simulated PXRD pattern based on the single crystal **2**, the as-synthesized and that after irradiated by LED light with the power of 3 W (460-465 nm).

6. In-situ UV-Vis Diffuse Reflection Spectroscopy

Optical diffuse reflectance spectra were measured at room temperature on a Perkin Elmer Lambda-950 UV/Vis/NIR spectrophotometer. The sample was irradiated by LED light with power of 3 W (460-465 nm) for different illumination time.

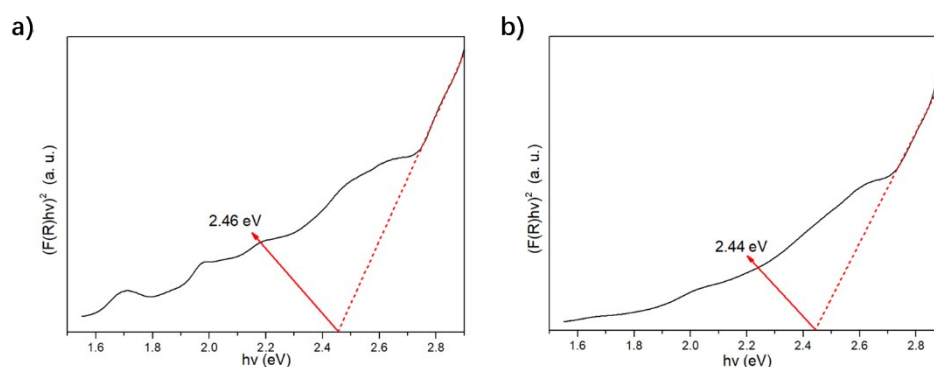


Figure S5. The estimated energy band gap for compound **1** (a) and **2** (b) by the UV/Vis diffuse reflectance spectroscopy based on the Kubelka-Munk Function.

7. Computational Studies

We calculated the electronic band structures of compounds by using the Vienna ab initio simulation package (VASP)^[S5,S6] and Perdew-Burke-Ernzerhof (PBE)^[S7] type generalized gradient approximation (GGA). The projector-augmented-wave (PAW) method^[S8] is used for the ionic pseudo-potentials. Monkhorst-Pack meshes^[S9] of (3×1×3) and (5×5×2) were used to sample the reciprocal space for compound **1** and **2**, respectively. The energy cutoff and convergence criteria for energy and force were set to be 520 eV, 1×10⁻⁷ eV, and 0.01 eV/Å, respectively.

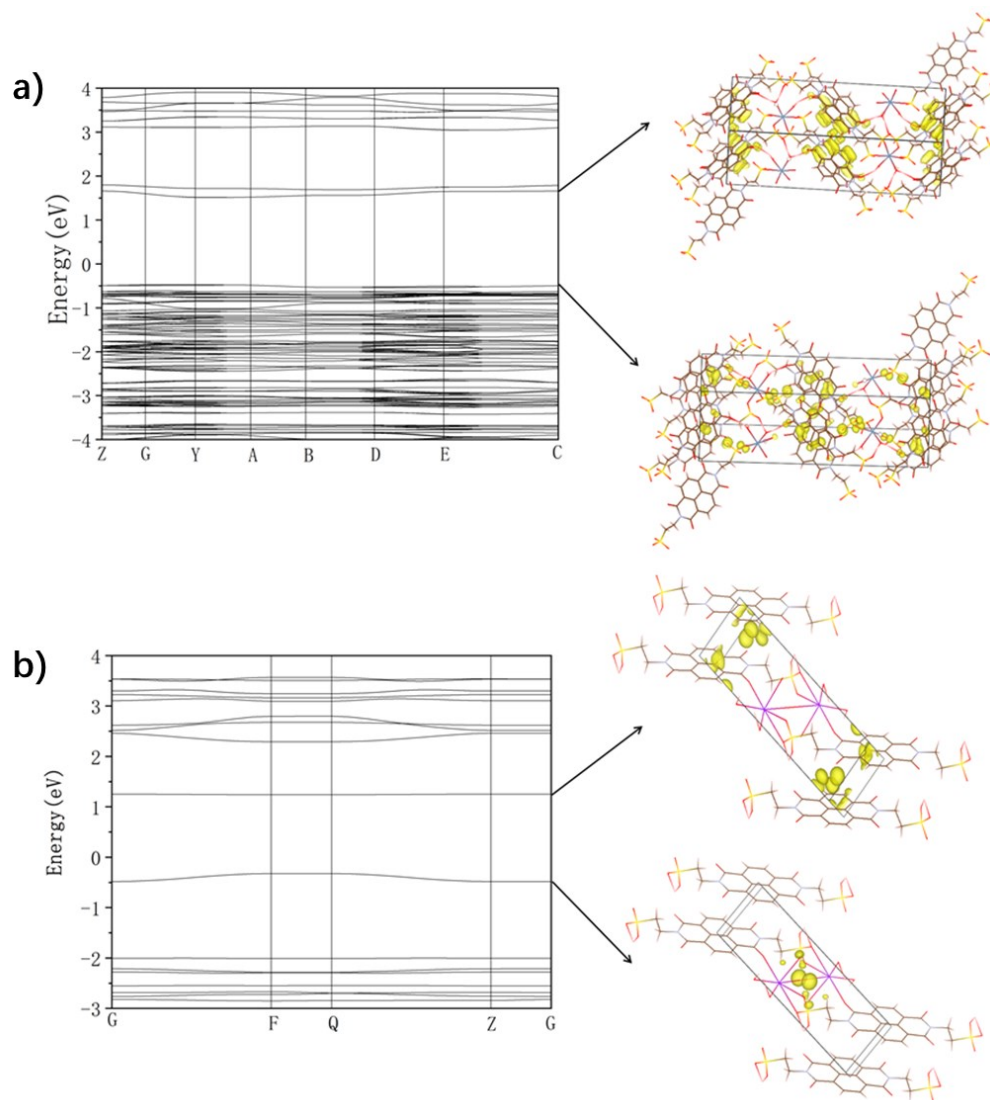


Figure S6. The electronic band structures for **1** (a) and **2** (b); Fermi level located at 0 eV.

The charge transfer interactions were also confirmed from the results of powder X-ray diffraction (PXRD) experiments and computational studies. All of the major peaks in the PXRD pattern of the darkened sample matched well with those of the fresh yellow sample, and both of these patterns coincided with the simulated one based on single-crystal data (Fig. S4). These results provided evidence for the photochromic behaviors of **1** and **2** having been caused by the formation of organic radicals rather than by structural changes. Furthermore, inspection of the

electronic band structure of **1** (see also that of **2** in Fig. S6b), which was calculated using the Vienna ab initio simulation package (VASP) program,^{S8} showed the radical-doped material having displayed the characteristics of a narrow band-gap and a donor–acceptor structure. Band gaps of **1–2** based on the Kubelka–Munk function were estimated from their UV-Vis diffuse reflectance spectra to be 2.46 and 2.44 eV, respectively (Fig. S5), values in reasonably good agreement with the calculated values of 1.80 and 1.60 eV, respectively. The results based on the electronic band structures indicated the precise charge transfer interactions and donor–acceptor structures in **1** and **2**. The electron-deficient imide rings of TauNDI were also found to serve as the predominant contributors to the lowest conduction bands, and oxygen atoms from sulfonic acid were found to act as the main contributors to the highest valence bands, consistent with the results of structural analysis. TauNDI molecules acted as electron acceptors as well as electron donors. Introduction of a donor and acceptor into the material at the same time not only favored the formation of charge transfer interactions but also stabilized and increased the lifetimes of the resultant organic radicals, which has been demonstrated elegantly for these compounds. The hydrogen bond, lone pair– π and C–H--- π interactions were indicated to provide effective pathways for the transfer of charge between the components of the compounds, and to a certain extent, the degree of charge transfer of a crystalline material can be adjusted and controlled by providing external photostimulation.

8. Antibacterial Test

Six different strains of bacteria including laboratory-sensitive strains (*Staphylococcus aureus* ATCC6538, *Pseudomonas aeruginosa* ATCC9027, *Bacillus subtilis* CMCC63501, *Escherichia coli* BL21(DE3)) and clinically isolated MDR bacteria (*Staphylococcus aureus* T23 and *Pseudomonas aeruginosa* P53, abbreviated to MRSA and MDR-PA, respectively) were chosen for evaluating the antibacterial activity of the three ultrastable radical-doped compounds. All the bacteria were cultured in the Nutrient-Broth (NB) medium at 310 K under shaking (250 rpm/min). The exponential growth bacteria and UV sterilized compounds were transferred to 3 ml liquid NB medium at the ratio of 1% (V/V) and 0.05% (m/V), respectively. Visible light irradiation tests were conducted for 1 h before incubating in the 310 K bacteriological incubators for 6 h. And then the same set bacteria suspensions were serially diluted to the same appropriate proportion with PBS (10 mM, pH 7.4). A 100 μ l portion of the dilution with bacteria was spread on the solid NB agar plate, and colonies formed after 16 h incubation at 310 K were counted. The inhibition ratio was determined by dividing the number of colony-forming units (CFU). The inhibition ratio (IR) was calculated according to the equation below:

$$IR = \frac{C_i - C_a}{C_i} \times 100$$

Where C_a is the CFU of the experimental group treated with light (or not) in the presence of radical-doped compounds, and C_i is the CFU of the control group without compounds.

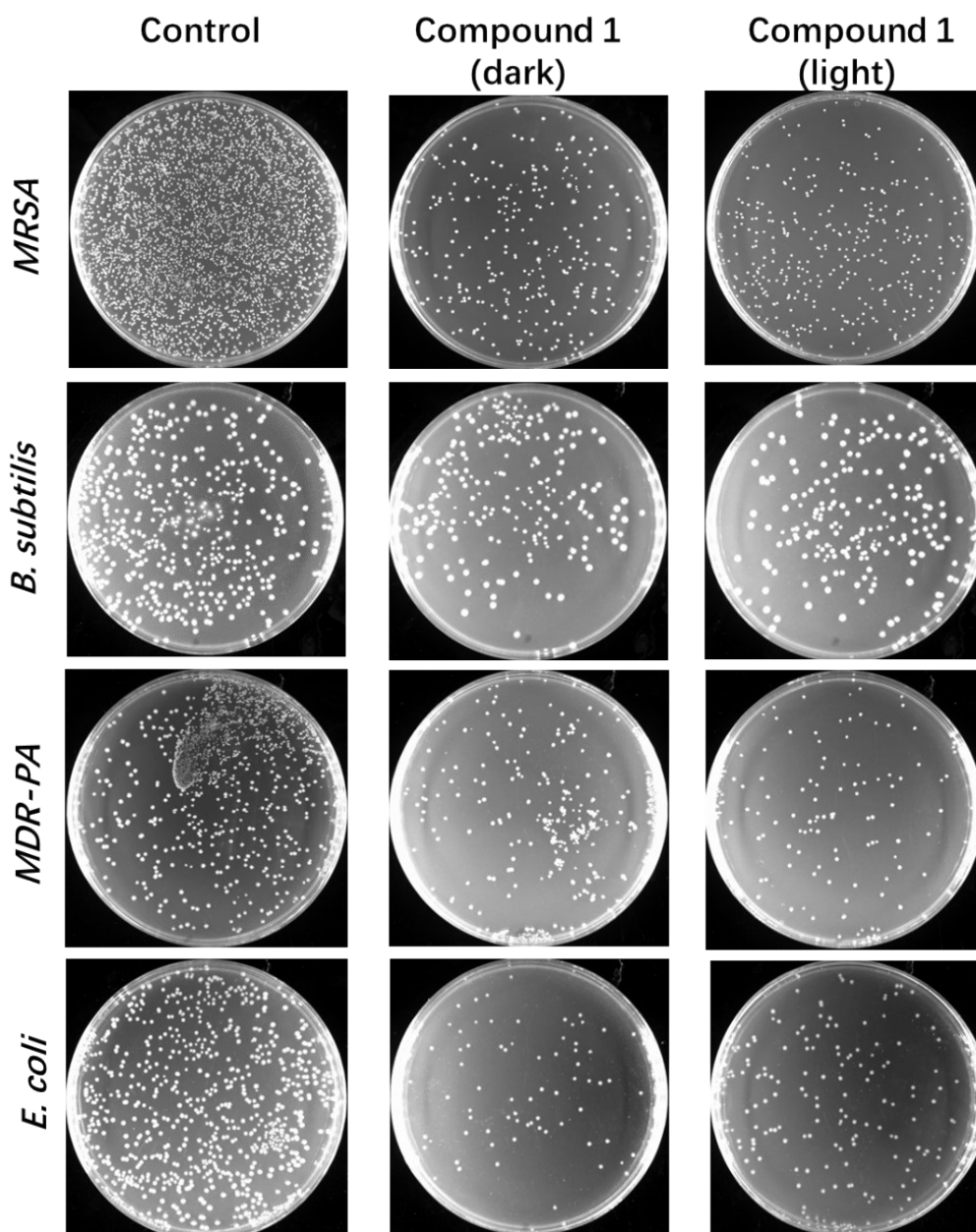


Figure S7. Colony forming units (CFU) for **MRSA**, *B. subtilis*, **MDR-PA** and *E. coli* treated with radical-doped compound **1** under exposing dark or light. The bacterial samples without treatment of radical-doped compounds as the control.

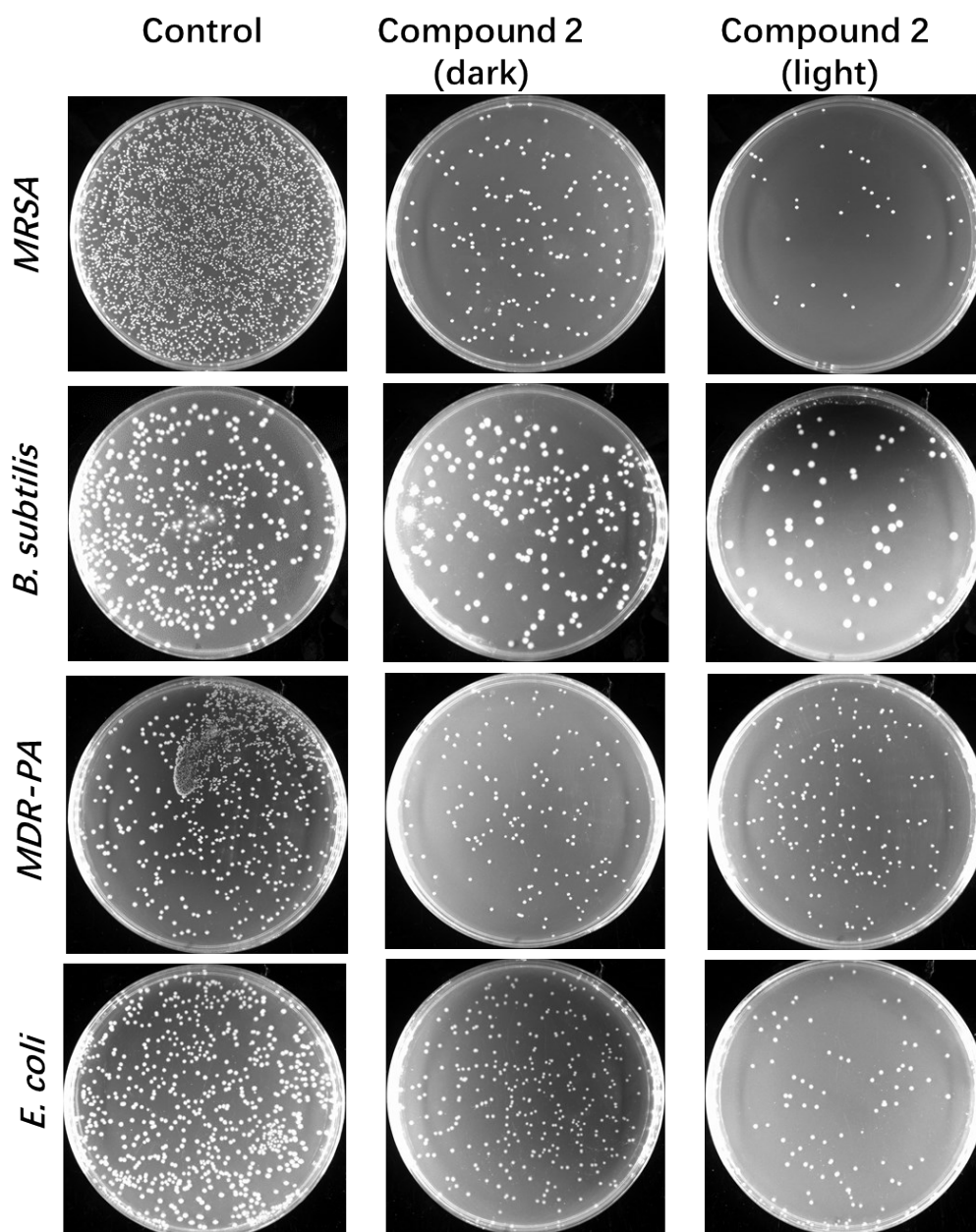


Figure S8. Colony forming units (CFU) for **MRSA**, *B. subtilis*, **MDR-PA** and *E. coli* treated with radical-doped compound **2** under exposing dark or light. The bacterial samples without treatment of radical-doped compounds as the control.

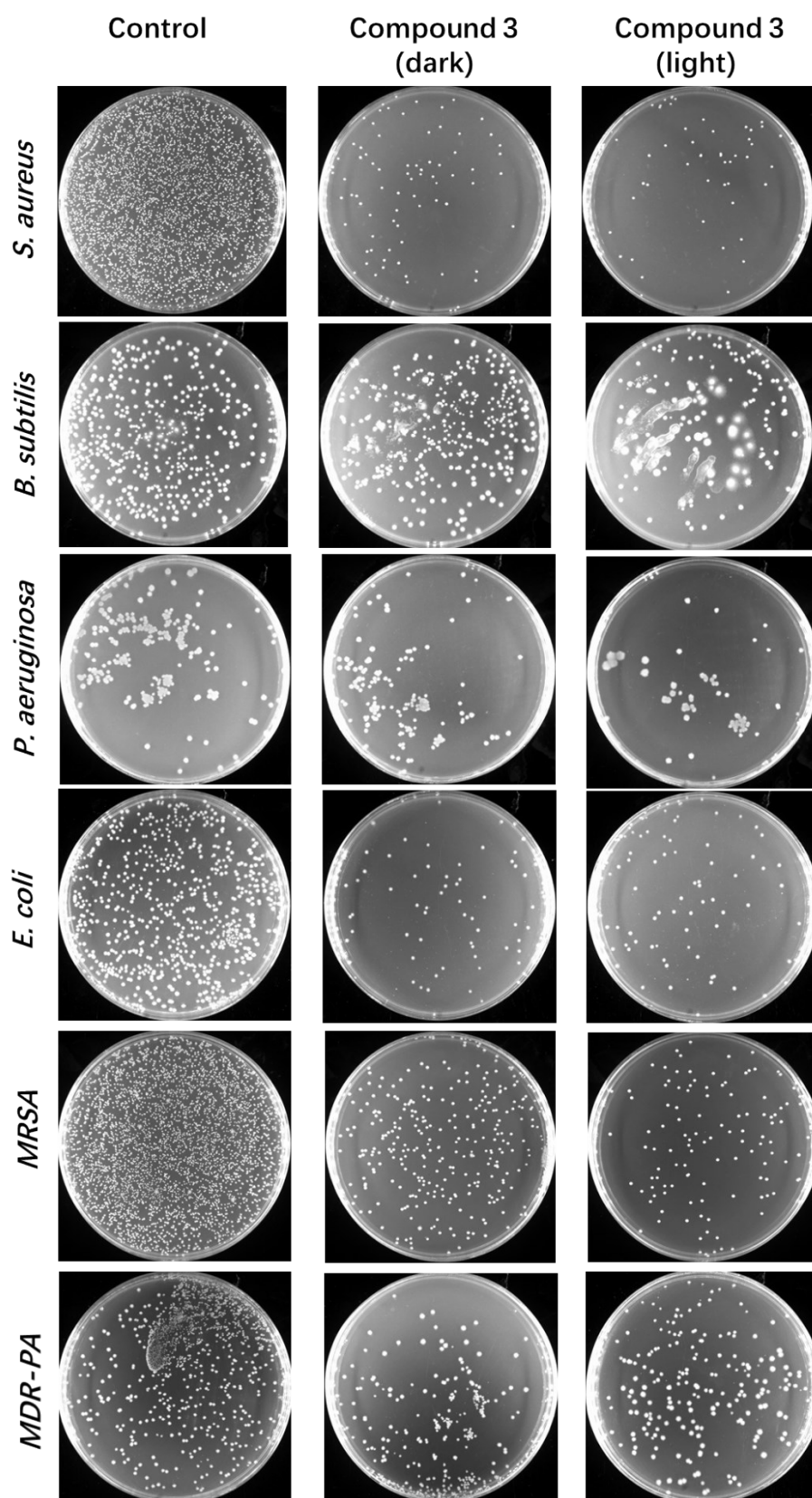


Figure S9. Colony forming units (CFU) for *S. aureus*, *B. subtilis*, *P. aeruginosa*, *E. coli*, **MRSA** and **MDR-PA** treated with radical-doped compound **3** under exposing dark or light. The bacterial samples without treatment of radical-doped compounds as the control.

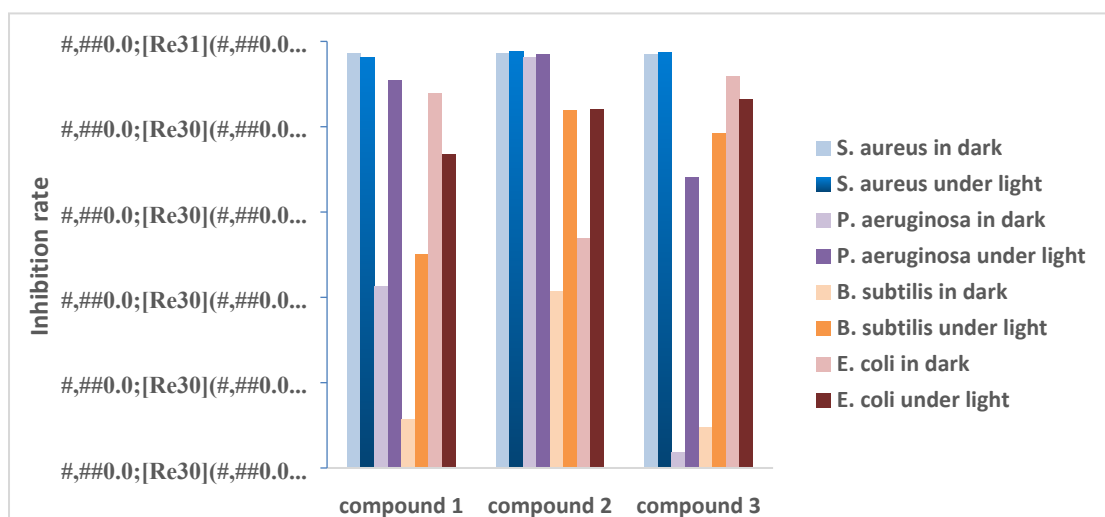


Figure S10. Column graphs of the colony inhibition ratio (IR) of *S. aureus*, *B. subtilis*, *P. aeruginosa* and *E. coli* with compounds **1-3** under dark or light irradiation.

9. Thermogravimetric Analyses

TGA of an air-dried sample of compounds **1** or **2** was conducted on a TGA/DSC 1 STAR^e system with a heating rate of 10 K/min under an N₂-atmosphere. Thermogravimetric analyses revealed that **1** and **2** exhibit relatively excellent thermal stability.

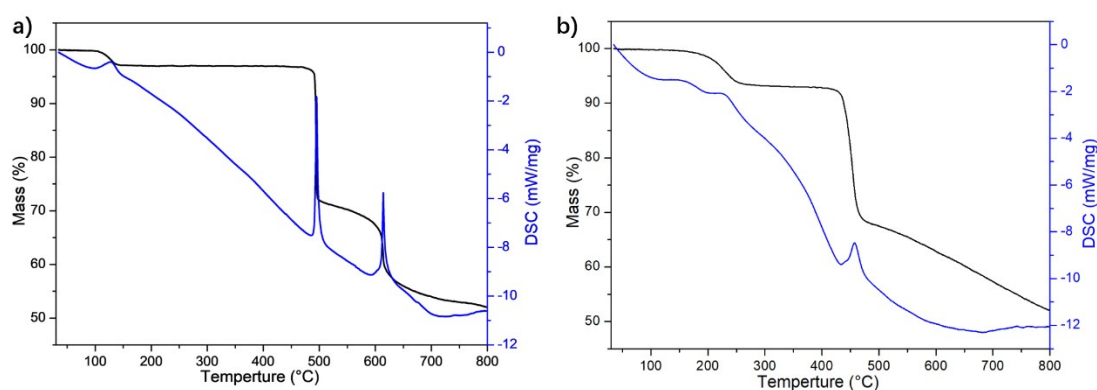


Figure S11. TGA/DSC curve of compound **1** (a) and **2** (b).

10. Reference

- S1 J. Z. Liao, J. F. Chang, L. Meng, H. L. Zhang, S. S. Wang, C. Z. Lu, *Chem. Commun.* **2017**, 53, 9701.
- S2 Dolomanov, O.V., Bourhis, L.J., Gildea, R.J, Howard, J.A.K. Puschmann H. *J. Appl. Cryst.*, 2009, **42**, 339.
- S3 Bourhis, L.J., Dolomanov, O.V., Gildea, R.J., Howard, J.A.K., Puschmann, H. *Acta Cryst.*, 2015, A71, 59.
- S4 Sheldrick, G.M. *Acta Cryst.*, 2015, **C71**, 3.
- S5. G. Kresse and J. Furthmüller. *Comput. Mater. Sci.*, 1996, **6**, 15.
- S6. G. Kresse and J. Furthmüller. *Phys. Rev. B*, 1996, **54**, 169.

S7. J. P. Perdew, K. Burke and M. Ernzerhof. *Phys. Rev. Lett.*, 1996, **77**, 3865.

S8. G. Kresse and J. Furthmuller. *Phys. Rev. B*, 1996, **54**, 11169.

S9. H. J. Monkhorst and J. D. Pack. *Phys. Rev. B*, 1976, **13**, 5188.